Canadian Nuclear Safety Commission | Commission canadienne de sûreté nucléaire

SKI STATENS KÄRNKRAFTINSPEKTION Swedish Nuclear Power Inspectorate

**CSSP Report 2004-01-03** **SKI Report ISRN SKI-R-03/47**

# FIELD TEST OF A DCVD USING AN IXON CAMERA WITH A LUMOGEN-COATED EMCCD DETECTOR

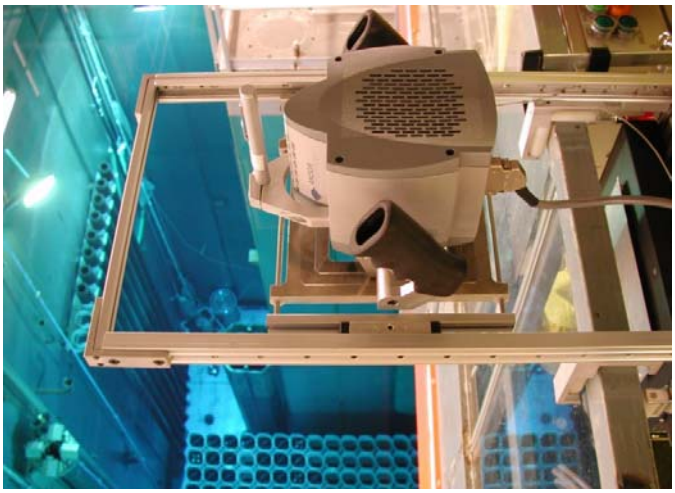

**Canadian and Swedish**
**Safeguards Support Programs**

# FIELD TEST OF A DCVD USING AN IXON CAMERA WITH A LUMOGEN-COATED EMCCD DETECTOR

Prepared for the Canadian Safeguards Support Program
and the Swedish Support Program

**J.D. Chen[1], A.F. Gerwing[1], R. Maxwell[2], M. Larsson[3], K. Axell[3], L. Hildingsson[3], B. Lindberg[4] and F. Vinnå[5]**

[1]Channel Systems Inc., 402 Ara Mooradian Way, Pinawa, Manitoba R0E 1L0, Canada
[2]Canadian Nuclear Safety Commission, 280 Slater Street, Ottawa, Ontario K1P 5S9, Canada
[3]Swedish Nuclear Power Inspectorate, Klarabergsviadukten 90, SE-106 58 Stockholm, Sweden
[4]LENS-TECH AB, Anbudsvägen 5, SE-931 64, Skellefteå, Sweden
[5]Teleca Design and Development, Telegrafgatan 8A, SE-169 84 Stockholm, Sweden

2003 December 2

**SKI: ISSN 1104-1374**
**CSSP TASK ID: DV011**
**IAEA TASK: JNT/A704**

CANADIAN NUCLEAR SAFETY COMMISSION AND
SWEDISH NUCLEAR POWER INSPECTORATE
DISCLAIMERS

ABSTRACT

The Canadian and Swedish Safeguards Support Programs have developed a new digital Cerenkov viewing device (DCVD) to verify spent fuel. The new system, based upon an electron-multiplied charge-coupled device that is lumogen coated, can operate at 14 frames per second using the fast 5 MHz analogue to digital converter. The new DCVD was successful in measuring the long-cooled Ågesta fuel with a burnup of 1200 MWd/t U and a cooling time of 31 years, which is well below the target of 10 000 MWd/t U and 40-years-cooled. Scanning of fuel assemblies was successfully demonstrated. With the aid of a laser pointer system, random verification within a reasonable time frame was also demonstrated.

Document Revision History

Revision 0 2003 December 2

# TABLE OF CONTENTS

# LIST OF FIGURES

# 1 INTRODUCTION

The digital Cerenkov viewing device (DCVD) has been further developed by the Canadian and Swedish Safeguards Support Programs to the stage that dynamic scanning of a row of spent-fuel assemblies to verify spent fuel is now possible. The first instrument developed in this program, the Concept SCCD Cerenkov viewing device (CVD)[1, 2, 3], demonstrated that using a low-noise, charge-coupled device (CCD) with ultraviolet light sensitivity had a number of advantages over the Mark IVe CVD. The detector used in the Concept system was lumogen coated and had an ultraviolet (UV) light quantum efficiency of 8%. This study indicated that a detector with higher efficiency was required to verify the weak Cerenkov glow from the target of 10 000 MWd/t U, 40-year-cooled spent fuel.

A slow-scan prototype DCVD was developed next to meet the measurement objective. The camera, manufactured by Andor Technology, incorporated a Marconi back-thinned, UV-enhanced, 1024 x 1024 frame-transfer CCD with a UV quantum efficiency of 52%. Additionally, a portable computer based upon the PC/104-*plus* format, a backpack to hold the computer, a hardware user interface (HUI), liquid crystal display (LCD), head-mounted display (HMD) and a railing bracket were developed and fabricated. The prototype DCVD was field tested at the Swedish Central Interim Storage for Spent Fuel (CLAB) on pressurized-water reactor (PWR) fuel and non-fuel, long-cooled boiling-water reactor (BWR) fuel and long-cooled Ågesta test reactor fuel assemblies[4]. A second field test was carried out at Oskarshamn Unit 2 (BWR), Ringhals Unit 1 (BWR) and Ringhals Unit 2 (PWR) on fuel and non-fuel assemblies. These studies[4] provided valuable measurement experience in a number of nuclear facilities. The prototype DCVD with its high UV efficiency easily verified the target spent fuel.

This report presents the test results of a new high-speed digital camera system. The camera, manufactured by Andor Technology, consists of a 288 x 576-pixel lumogen-coated, electron-multiplied, charge-coupled device (EMCCD) and a 5 MHz analogue to digital converter in the camera head. The camera controller card is attached to an external PCI bus that interfaces with the computer through the PCMCIA port. The complete system is battery operated. A new, improved railing bracket and a laser pointing system for orientation was fabricated for the new camera system.

In November of 2002, this high-speed DCVD was field tested in Sweden at Oskarshamn Unit 2 on BWR spent-and non-fuel assemblies and at CLAB on PWR spent-and non-fuel assemblies, long-cooled BWR spent fuel and long-cooled Ågesta test reactor fuel. Cerenkov images produced by the DCVD are given in this report. In addition, experience on fuel inventory verification using random and 100% sampling is discussed.

# 2 INSTRUMENTATION

The DCVD consists of a CCD camera (Andor Technology Inc., Belfast, Northern Ireland), a controller card, an external PCI bus system manufactured by Magma, a ViewSonic tablet computer, a railing bracket to hold the system and a laser pointing system to orient the camera. Windows XP is the operating system for the computer and DCView is the software developed for the DCVD. The schematic of the overall equipment is shown in Figure 1. Cerenkov light passes through the objective lens and a UV-pass filter to produce an image on the CCD located in the detector vacuum housing. The camera head contains a three-stage thermoelectric (Peltier) cooler, a pre-amplifier, an analogue-to-digital

converter (ADC) and control electronics. The Magma chassis contains the external PCI bus and the Andor controller card. The Magma box is powered by two lithium-ion batteries, which supply power for the camera system and the Magma box. The two batteries are capable of powering the camera system at a chip temperature of –20°C for 3 hours. Under normal operating conditions the computer battery has the capacity to operate for more than 2 hours. A 512-MB memory stick is used to transfer data from the ViewSonic Computer.

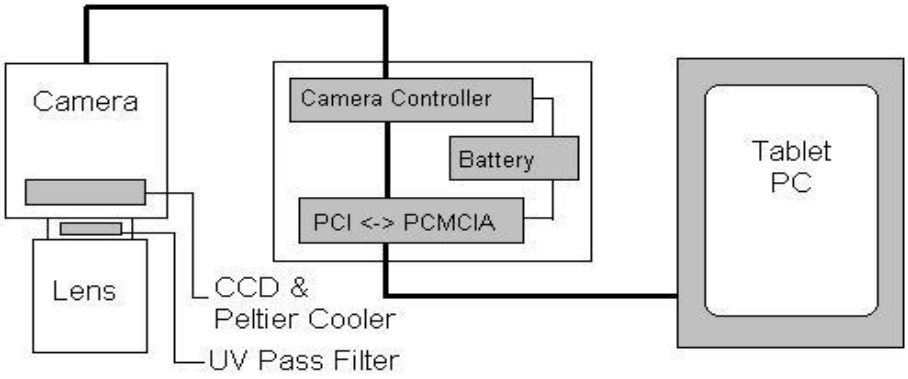


*Figure 1: Data acquisition system used to obtain Cerenkov images*

Figure 2 shows pictures of the DCVD instrument and the 105-mm lens used in imaging PWR fuel assemblies. The longer 250-mm lens was used to image the smaller BWR and Ågesta fuel assemblies.

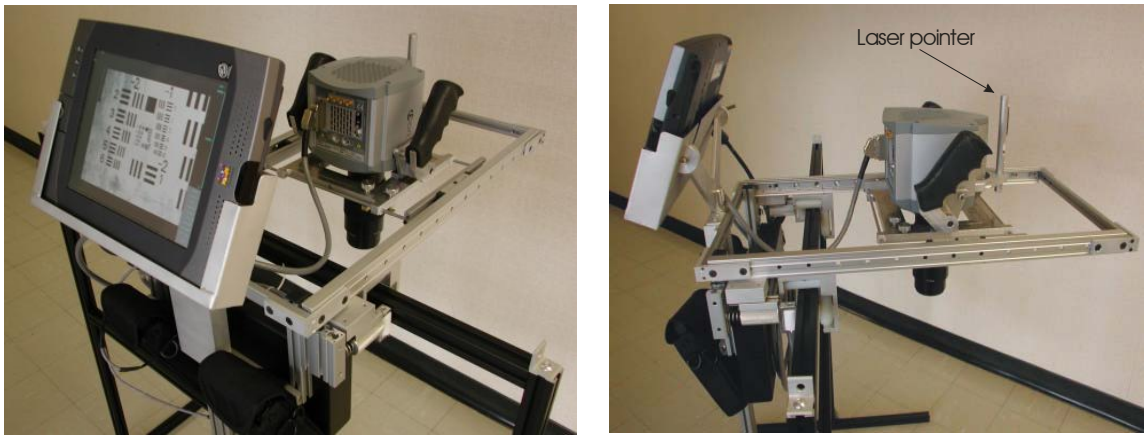


*Figure 2: DCVD instrument*

## 2.1 Railing bracket and laser pointer

Figure 2 shows the laser pointer mounted on the front of the camera head. The 5-mW laser emits bright green light at 532 nm that can be seen at the bottom of the fuel bay through 15 m of water. The Andor camera was mounted on a platform with a gimbals system that permitted tilting of the camera head in two directions for precise alignment over a specific fuel assembly. The railing bracket could be moved along the length of a bridge and, additionally, the platform could be moved small distances in the x and y direction for fine positioning over the fuel assemblies.

## 2.2 Computer and external PCI bus

The "tablet" computer used in the DCVD instrument is a ViewSonic ViewPad 1000 with an integrated touch screen liquid crystal display (LCD), shown in Figure 2. The 26.4-cm LCD screen has a resolution of 800 x 600 pixels. The touch screen feature permitted the DCVD imaging program, DCView, to be used without the need of a keyboard or pointing system. The computer has a 20 GB hard drive, 256 MB memory, one Type II PC slot, one Ethernet and two USB ports. The processor is an 800 MHz Intel® mobile Celeron®. An extended PCI bus manufactured by Magma was used to connect the Andor camera controller card to the computer via the PC card slot. The Magma and controller cards were housed in a separate box, which was attached to the railing bracket. Two 11-V lithium-ion batteries (Molicel®) supplied power to the two cards and to the Peltier cooler in the camera. The two batteries were able to power the system for nearly 3 h. Batteries can be changed during DCVD operation.

## 2.3 Graphical user interface

The DCView graphical user interface (GUI) is shown in Figure 3. A green, square region of interest (ROI) appears in the centre of the screen. In Auto-image mode, the image data within this region of interest is used to calculate the display brightness and contrast. The ROI is normally set to the size of a single fuel assembly for optimum operation. In the lower right-hand side is a status window, which shows the DCVD's current settings.

Figure 4 shows the menu system used to set up the camera operation. The menus are opened in sequence by touching the screen on the right hand side. One tap on the right hand side of the screen brings up the first menu, ***Camera, Display, File*** and ***Shutdown*** and tapping the top or bottom of the screen selects the menu item (blue band). If ***Camera*** operation is selected, a second tap on the right hand side of the screen brings up the second menu: ***Acquisition, Exp.*** *(exposure)* ***Time, Binning, Gain, Temp.*** *(temperature)* and ***Zoom***. A specific camera operation can be selected by tapping the top or bottom of the screen. ***Acquisition*** is selected here and a third tap on the right hand side of the screen brings up the next menu, which gives the ***Acquisition*** options of ***Run, Still*** and ***Single***. To back out of the menus to provide an unimpeded view of the image, the left side of the screen is tapped a number of times until all the menu items have disappeared from view.

An intensity bar on the right-hand side of the screen registers the intensity of the measured fuel assembly (ROI). The numerical value is shown in the status bar (16500 in Figure 4).

## 2.4 Charge-coupled device and camera head

The detector used is a Marconi CCD65 frame-transfer chip with a lumogen coating to provide UV light sensitivity. The active area of the chip consists of an array of 576 x 288 rectangular pixels, each 20 x 30 μm, with an overall dimension of 11 x 8.5 mm. Each pixel is a semiconductor detector element. The lumogen coating on the CCD converts the incident UV photons to photons with a wavelength of about 530 nm (yellow). These incident photons create ion-pairs within the pixels (only the electron within the pair is generally referenced). The electrons are accumulated for a pre-selected integration time and then shifted, line by line, to the masked area in the chip (Figure 5). The charge in each pixel of each row is then shifted to a readout register. The charge is transferred to the gain register where an additional charge is added to each pixel (gain). This new gain feature is

called an electron multiplied charge-coupled device (EMCCD). The charge is then amplified and converted to a digital number through the 5 MHz analogue to digital converter. All these operations are carried out in the camera head. The digital data is transferred through the Andor controller card and PC Card bus to the program's memory locations.

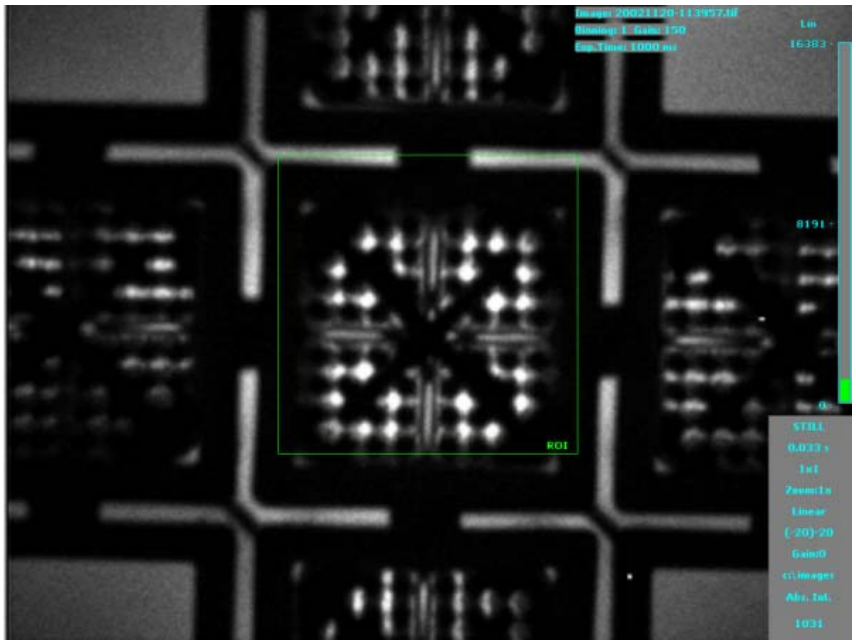


*Figure 3: Graphical user interface, menus hidden*


*Figure 4: Graphical user interface menu system*

The shift process that transfers charge during the frame transfer step and during the readout step can be performed any number of times for each readout, which effectively sums the charge in adjacent pixels. This process is known as "binning". For example, in one

common mode two lines are transferred and summed into the readout register, which is then transferred to the gain register. From there, two pixels at a time are moved into the charge detection node. This example would "bin" four pixels into one "super pixel". The process results in better signal-to-noise ratios, a higher frame transfer speed, but less resolution.

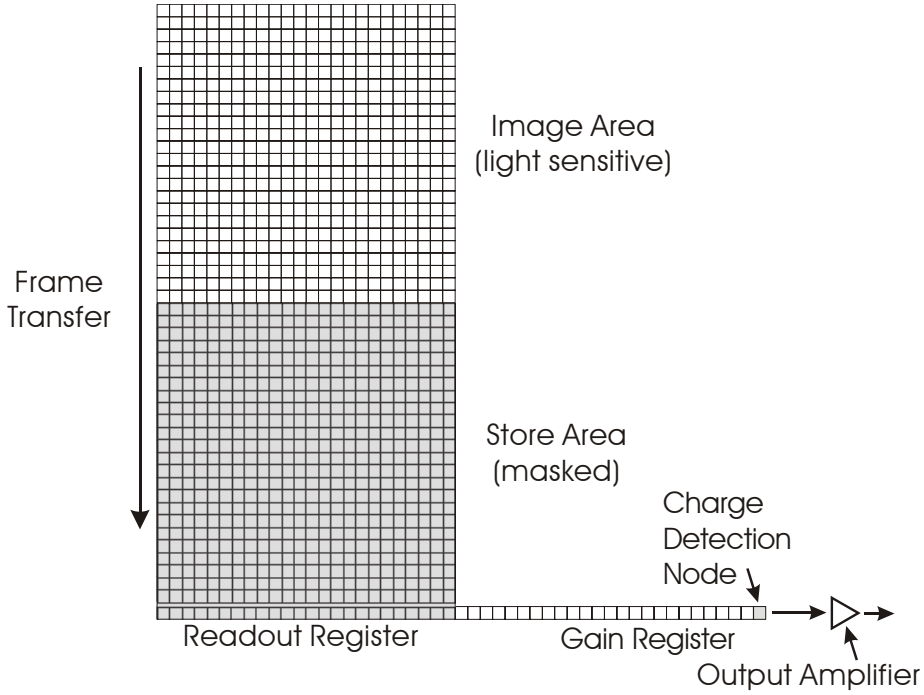


*Figure 5: Marconi CCD65 frame transfer chip*

The quantum efficiency of the chip was measured at 310 and 660 nm. A calibrated International Light IL1800 radiometer was used to measure the photon flux at the CCD detector. The measured quantum efficiencies at 310 and 660 nm, respectively, are 8.5% and 30%. There were no factory-measured quantum efficiency data but data from generic curves give values of 10 and 25% for these wavelengths.

The dark current at -20ºC was 3 electrons per pixel per second, decreasing to 1.3 electrons per pixel per second at -40ºC. Andor measured a very low dark current of 0.035 electrons per second per pixel at -56ºC. Dark current at this temperature was not measured because the DCVD normally operates at -20ºC at exposures of less than 10 seconds, at which point noise is insignificant.

The measured CCD readout noise of ±39 electrons per pixel per second is almost identical to that obtained by Andor.

The camera head contains a three-stage thermoelectric cooler that can develop a -60ºC temperature differential from ambient. During the field tests, the detector was normally operated at -20ºC and took less than 3 minutes to stabilize.

### 2.5 Setup of equipment on the fuelling machine and walking bridge

The DCVD is shown mounted on a fuelling machine in Figure 6. The picture on the left shows a Cerenkov image of spent-fuel assemblies on the computer screen. The operator is setting camera parameters, (binning and exposure time) to optimize the image quality for

storage on the computer hard drive. The picture on the right shows the camera head mounted on the railing bracket with the laser pointer mounted in front of the camera head.

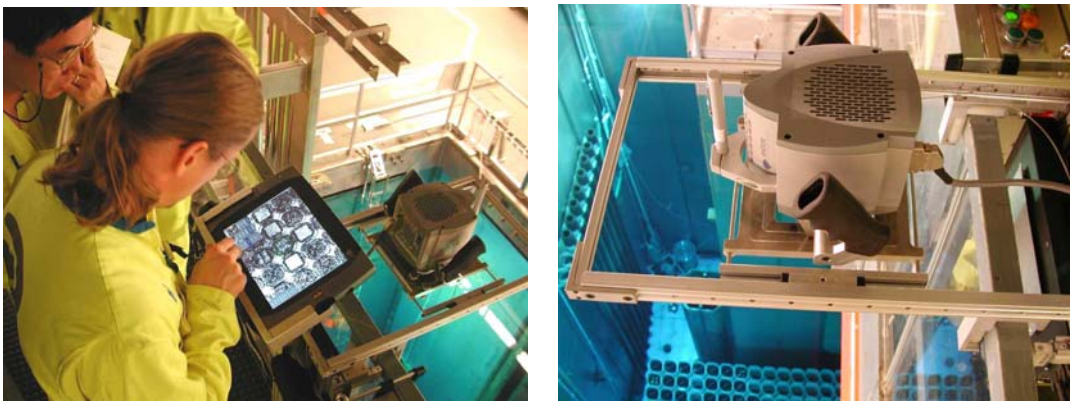

*Figure 6: The DCVD mounted on a fuelling machine*

The DCVD is mounted on the walking bridge in Figure 7. The laser pointer is on and two light spots are visible: one is a reflection off the surface of the water while the other is the reflection off the fuel assembly.

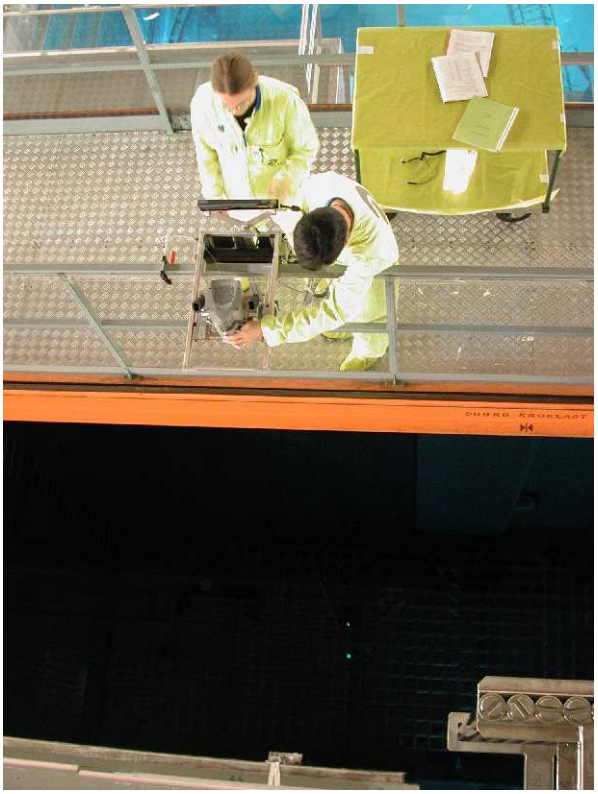

*Figure 7: The DCVD mounted on a walking bridge showing the laser beam*

## 3 EXPERIMENTAL RESULTS

The DCVD was tested at Oskarshamn Unit 2 on a variety of BWR spent fuels and a number of non-fuel assemblies. The measurement campaign also included measurements at

the CLAB fuel storage site on PWR fuel and non-fuel assemblies and several long-cooled BWR and Ågesta test reactor spent fuels.

The images shown in this report have been scaled to show optimum brightness and contrast. This is possible because of the digital nature of the images. Therefore, one must be careful when comparing images. A long-cooled spent-fuel Cerenkov image can look as bright as a short-cooled fuel even though the long-cooled fuel has less intensity (fewer counts). The only real measure of glow intensity is the actual pixel data itself. An algorithm to compute the intensity of the brightest pixels in the ROI is used to display the intrinsic intensity as a numeric value in the status bar and graphically in the right hand intensity bar shown in Figure 3.

A major difference between the prototype camera and the present camera is the higher frame rates of the new DCVD. This permitted faster focusing of the lens and the ability to dynamically scan fuel assemblies. The laser pointer permitted rapid location of specific fuel assemblies. This combination made random verification procedures feasible, which provides a benefit over the 100% verification procedure used with the Mark IVe CVD. The details of this experiment are given in Section 3.5.

### 3.1 Precision measurements

For the BWR fuel, the DCVD was aligned over the centre of a fuel arrangement that had fuels with similar burnup and cooling times set in a cross geometry. A PWR fuel assembly at CLAB was also selected for precision measurements. Ten measurements were taken of each fuel assembly with repositioning of the DCVD between measurements. The results are show in Table 1. For the higher intensity readings on the BWR assembly, precisions of 4.7% were obtained. Precision was somewhat lower, at 9.2%, for the less intense PWR fuel.

*Table 1: Precision measurements for PWR and BWR images*

| Reading # | BWR Intensity (counts) | | PWR Intensity (counts) | |
|---|---|---|---|---|
| 1 | 204 | | 117 | |
| 2 | 206 | | 119 | |
| 3 | 202 | | 97 | |
| 4 | 201 | | 115 | |
| 5 | 196 | | 127 | |
| 6 | 201 | | 109 | |
| 7 | 207 | | 127 | |
| 8 | 183 | | 123 | |
| 9 | 191 | | 135 | |
| 10 | 186 | | 128 | |
| Mean | 196.3 | | 119.7 | |
| Precision (1σ) | 9.27 | 4.7% | 10.95 | 9.2% |

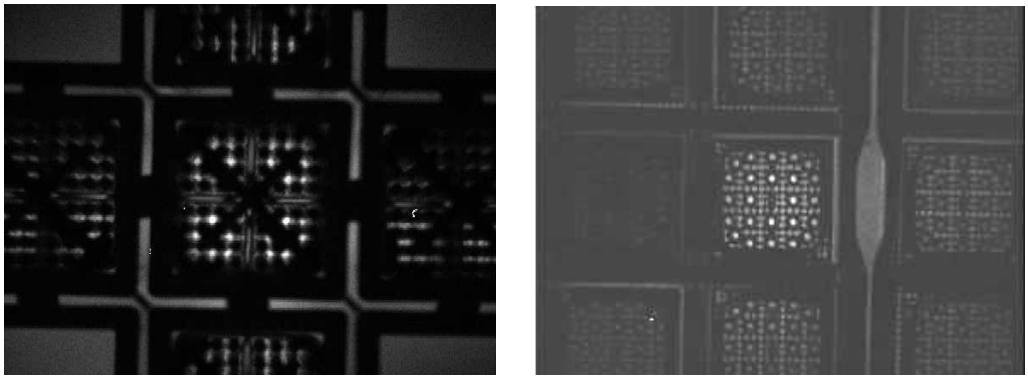

BWR PWR

*Figure 8: Images used for precision measurements*

### 3.2 BWR spent fuel with missing fuel rods

The Cerenkov image Figure 9(a) shows a number of missing fuel rods. Comparison with the normal fuel assembly shows that 9 rods can be readily detected as missing. The 10$^{th}$ missing rod is located under the centre of the lifting handle and cannot be seen in this view of the assembly.

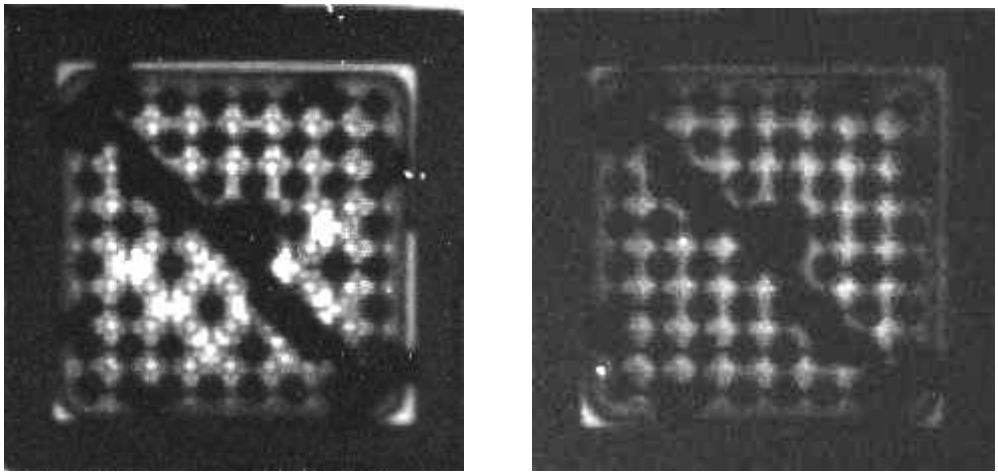

(a) 10 missing fuel rods (b) Normal fuel assembly

*Figure 9: BWR fuel assembly with and without missing fuel rods*

### 3.3 Scanning BWR fuel arrangements with non-fuel assemblies

The skeleton assembly appears to emit Cerenkov light because it is surrounded by short-cooled spent fuel. The gamma radiation from the surrounding fuel travels into the volume of water occupied by the skeleton assembly and generates Cerenkov light. The DCVD mounted on the walking bridge was moved across this fuel arrangement containing non-fuel assemblies at 8 frames per second. The skeleton non-fuel assembly shown in Figure 10 was readily detected as a non-fuel item at this frame rate.

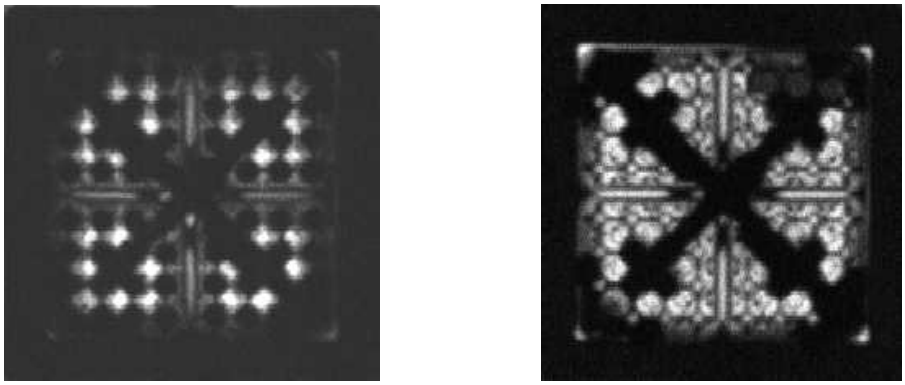

(a) SVEA fuel 1-year-cooled (b) Skeleton

*Figure 10: Skeleton non-fuel assembly surrounded by one-year-cooled fuel*

The high-density non-fuel and long-cooled (16 000 MWd/t U, 21-year-cooled) fuel assemblies shown in Figure 11 are surrounded by relatively short-cooled fuel. In the scanning mode of operation, these fuel assemblies were difficult to verify because they had very weak glow intensities (i.e. low count rates). With 8-second time exposure images, however, the high-density non-fuel assembly exhibited the different Cerenkov glow characteristics expected of non-fuel assemblies. In the long-cooled fuel assembly, highly collimated light from between the fuel rods was clearly seen; this was not detectable in the high-density non-fuel assembly.

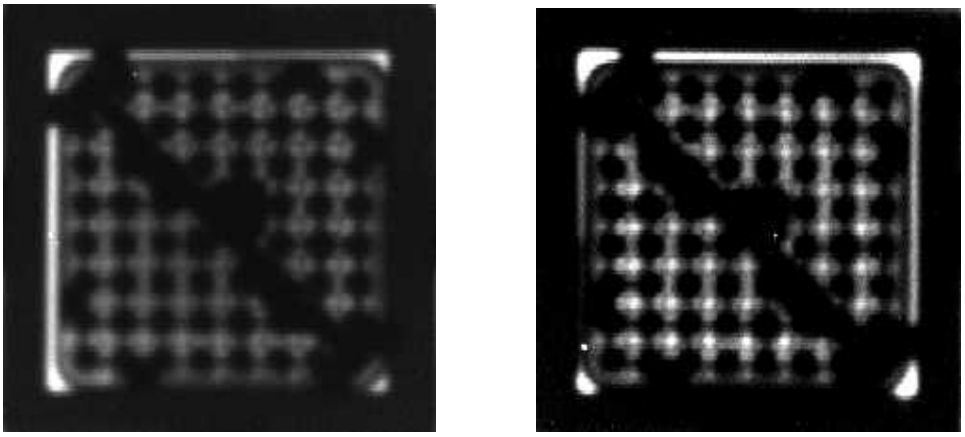

(a) High density 8 x 8 BWR non-fuel (b) BWR long-cooled fuel

*Figure 11: High-density non-fuel and long-cooled assemblies (surrounded by short-cooled fuel)*

### 3.4 Scanning PWR fuel arrangements with non-fuel assemblies

It was difficult to verify the helium non-fuel assembly (Figure 12) when surrounded by short-cooled near neighbours. This non-fuel assembly could be detected in scanning mode by watching the light from the guide tubes decrease at a slower rate than the short-cooled and long-cooled spent fuel. The light from all the guide tube holes in the helium non-fuel

assembly appears to be of the same intensity. The short-cooled and long-cooled spent fuel showed noticeably brighter inner guide tubes.

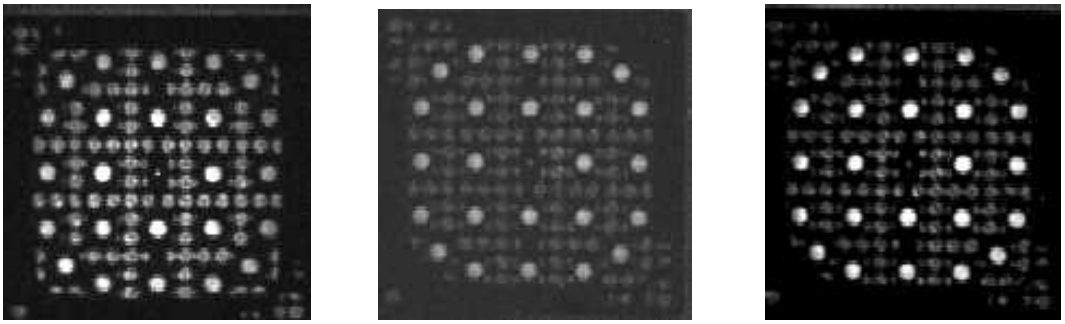

(a) 47 000, 5-year-cooled (b) Helium non-fuel (c) 20 000, 18-year-cooled

*Figure 12: Helium non-fuel assembly (surrounded by short-cooled fuel)*

The high-density non-fuel assembly (Figure 13) was easily detected in the scanning mode of operation. This assembly is the darkest of three PWR non-fuel assemblies studied. The intensity of light from the centre guide tubes is significantly lower than the outer guide tube holes. This is consistent with the near-neighbour effect where the gamma radiation from the near neighbours causes the outer guide tubes to have higher intensity than the inner guide tube holes. The high-density rods absorb the gamma rays as they pass through the assembly, resulting in a lower gamma flux in the central region of the assembly. The lower gamma flux in turn produces a lower Cerenkov intensity in the inner guide tube holes.

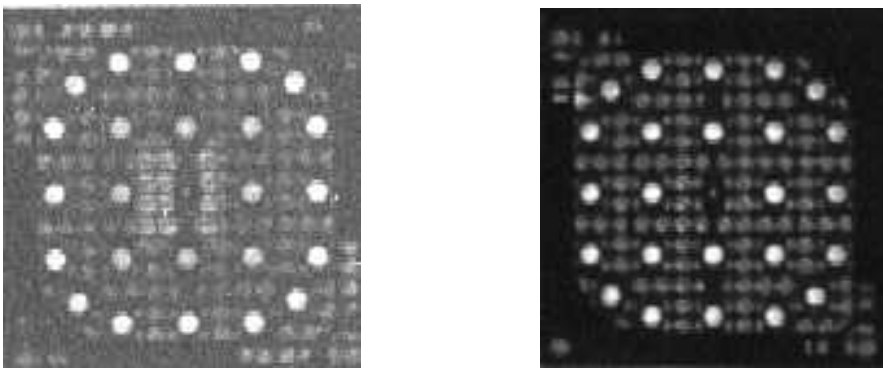

(a) High density non-fuel (b) 20 000 18-year-cooled

*Figure 13: Non-fuel (high density) and spent-fuel assemblies*

The skeleton non-fuel assembly (Figure 14) was easily verified in scanning mode. The image clearly shows that there are no fuel rods present. The outer and inner guide tube holes appear to show the same light intensity, which is unlike the spent fuel shown in (b). This is the brightest non-fuel assembly because it contains very little gamma-absorbing material.

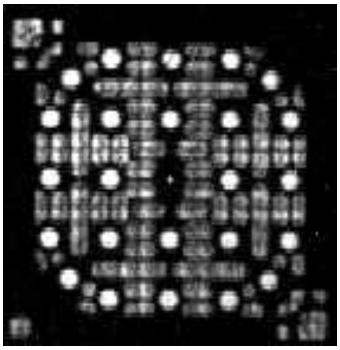

(a) Skeleton non-fuel

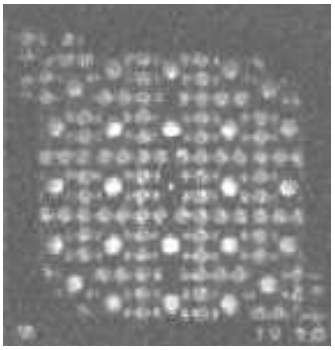

(b) 34 000, 16-year-cooled

*Figure 14: Non-fuel (skeleton) and spent fuel assemblies*

### 3.5 Spent-fuel verification exercise

*BWR Spent Fuel*

Two IAEA procedures were used to assess the capability of the DCVD for pond verification: random verification and 100% verification. The random verification procedure is described below. The 100% verification procedure is simply the verification of all fuel assemblies in the fuel storage pond.

There were 221 fuel assemblies in the pond to be verified. These assemblies have an average of 1.7 kg of Pu. Using a detection probability of 50% we can calculate[1] that 30 fuel assemblies must be verified. The fuelling-machine bridge was used for both exercises since it would be a more stringent test of the DCVD than the walking bridge.

The DCVD was set to 1/15 second exposure time and 2 x 2 binning. The higher binning has lower resolution but permits rapid scanning of the assemblies. The laser pointer was used to orient the DCVD over the required fuel assembly as specified on the pond map. Images of 12 specified fuel assemblies were saved to simulate an actual verification exercise. The random verification procedure took 45 minutes to complete while the 100% verification procedure took 82 minutes, which included saving images of the same 12 fuel assemblies. Time exposures from 1 to 10 seconds (at no binning, for highest resolution) were used to save images. Much of the time was used in resetting the DCVD from one mode and exposure time to another. Implementing some form of shortcut in the DCView user interface could significantly decrease the verification times.

*PWR Spent Fuel*

Two procedures were again used to assess the capability of the DCVD: random verification and 100% verification. The fuel bay contained 300 fuel assemblies with an average of 4.8 kg of Pu in each assembly. Using the previous formula, we can calculate that 102 fuel assemblies should be verified. Images of ten specific fuel assemblies were saved. A walking bridge was the only bridge available in the storage bay. The time taken for the random sampling procedure was 43 minutes, while the 100% verification procedure took 80 minutes. The PWR and BWR verification exercises took about the same time to complete but almost 3 times as many PWR assemblies were verified as BWR assemblies.

[1] $n = N\,(1-.051^{1.7/8})$ where N is the total number of fuel assemblies in the pond and n is the number of assemblies to be verified.

Because of the ability to quickly orient the DCVD over a specified fuel assembly, the random verification procedure was faster than the 100% verification procedure. This is contrary to the CVD method where the random verification procedure usually takes almost twice as long as the 100% verification procedure. The higher verification speed of the DCVD can be attributed to the laser pointer system, which permits fast orientation over a specific fuel assembly.

### 3.6 DCVD verification of long-cooled fuel

The graph shown in Figure 15 provides the photon flux at a measurement point above the fuel assembly as a function of burnup and cooling time. The target photon flux that the DCVD must meet is shown on the graph along with photon flux intensities of two fuel assemblies that are below the target fuel.

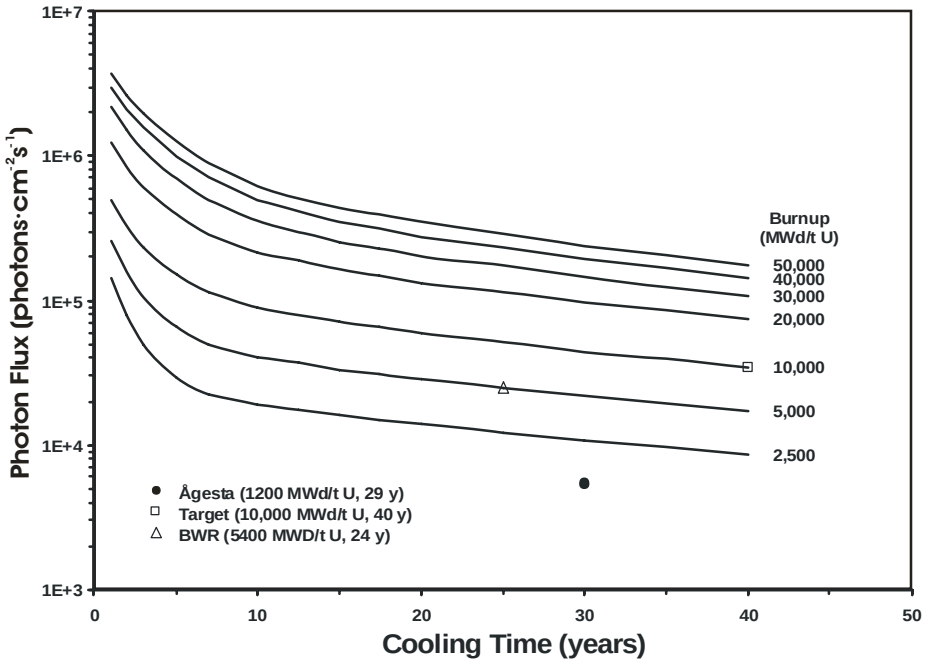


*Figure 15: Calculated photon flux emitted by a spent-fuel assembly as functions of burnup and cooling time*

*BWR Fuel*

The oldest (26-year-cooled) and lowest burnup (5400 MWd/t U) fuel at CLAB was measured by the DCVD. In Figure 16(a) the image was obtained at 4 x 4 binning with an exposure of one second. At this level of binning the general features can be detected but resolution is lacking and the fuel rods do not look round. This is contrasted with the unbinned image in Figure 16(b) taken with an 8-second exposure. The fuel rods are well resolved and highly collimated light from between the fuel rods can be clearly seen.

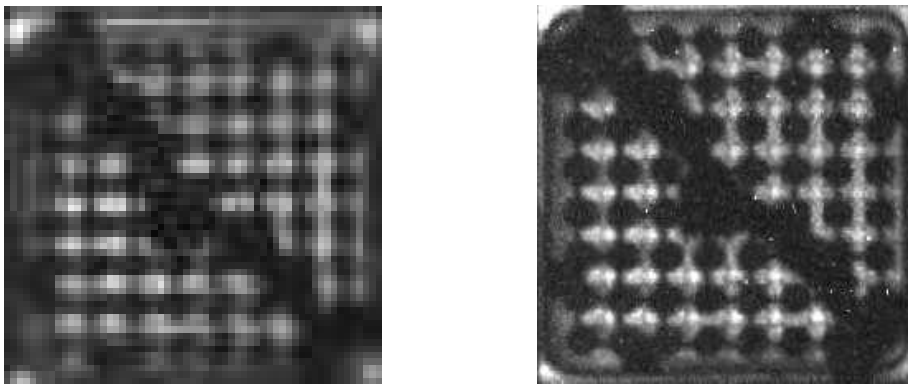

(a) 4 x 4 bin, 1 s (b) 1 x 1 bin, 8 s

*Figure 16: Long-cooled BWR fuel assembly*

*Ågesta Fuel*

The longest-cooled fuel assemblies at CLAB are from the Ågesta test reactor. Burnups are as low as 1200 MWd/t U with 31 years cooling time. Figure 17(a) shows a visible light picture of a basket containing 31 Ågesta spent-fuel assemblies. A normal camera image of a fuel assembly at 1200 MWd/t U, 31 years cooled is shown in Figure 17(b). Figure 17(c) shows the DCVD image of this fuel. The glow from between the fuel rods can be clearly seen and is quite uniform, a feature that can only be obtained after careful alignment above the fuel assembly. This is indicative of the high collimation of light from spent fuel. The intensity of this fuel assembly is 6.5 times lower than that emitted by the target fuel (10 000 MWd/t U and cooled for 40 years).

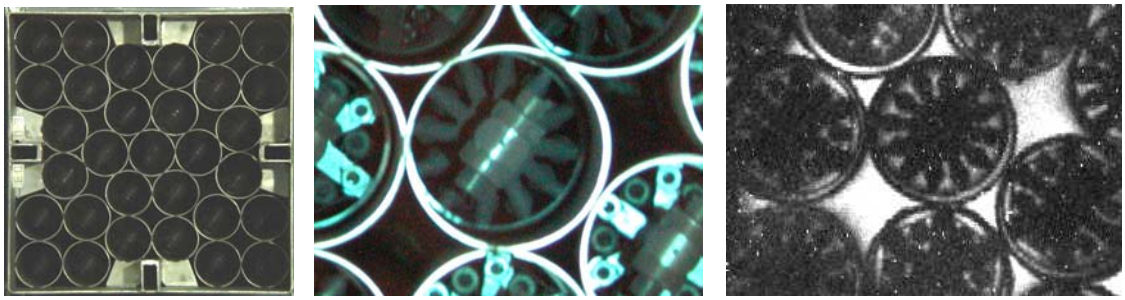

(a) Normal camera view (b) Close up of fuel (c) DCVD image, 2 x 2 bin, 8 s

*Figure 17: Ågesta fuel assembly 03052*

# 4 DISCUSSION

## 4.1 Ergonomics of the DCVD

The iXon camera system mounted on the railing bracket worked well on the walking and fuelling machine bridges. The time taken to remove the equipment from its transport case to mounting it on a bridge was less than 30 minutes. Scanning along the whole length of the walking bridge presented no problems. It was discovered that the walking bridge was not exactly parallel to the rows of fuel. Adjustments had to be made for alignment over specific fuel assemblies. The fuelling-machine bridge was more confined and there were fewer areas where the DCVD could be mounted. However, it was possible to view all of the fuel

assemblies from two sides of the fuelling machine. The laser pointer was invaluable in locating specific fuel assemblies.

Areas for improvement were identified. The railing bracket needed several tools to make adjustments for bridges with different geometries (e.g., top rail with round and square stock). Only one tool should be required for this operation. The number of different tools needed should be reduced by using appropriate thumbscrews or hand fasteners. Clearances for assembled parts were too small for certain parts. For example, fitting the computer mount to the bracket was difficult. Larger clearances are required to allow shorter assembly times. The gimbals platform design allowed a twisting moment when moved. A redesign is required to make the motion more direct so that the camera platform cannot twist when moved.

### 4.2 Computer, LCD, external PCI bus and batteries

The tablet computer, an external PCI bus for the iXon controller card and battery operation made the DCVD portable. The camera and electronics were powered with two lithium-ion batteries, which operated for ~3 hours. These batteries could be changed while the DCVD was in operation. The computer was powered by its own battery, which lasted for ~2 hours. The system had to be shut down to replace the computer battery.

A two-hour battery life for the computer was not sufficient for research and development work. It may, however, be adequate for inspection purposes where the time for fuel verification is often less than two hours. Tablet computers are a recent development and computers with battery lives of >4 hours may soon be available.

Control of the camera head detector operations and communication with the computer is achieved through a custom-built controller card. The camera head obtains power for the thermoelectric cooler and sends its digital data to the computer via this controller card. Andor is working on ways to eliminate this controller card, replacing it with high-speed ports such as USB2. A separate cable may still be required to power the thermoelectric cooler.

### 4.3 Sensitivity and scanning

Laboratory measurements have indicated that the prototype DCVD is 100 times more sensitive than the Mark IVe CVD. The present detector (on-chip gain and lumogen coating, 8.5% QE at 300 nm) was tested empirically against the prototype system (back-thinned, 52% QE at 300 nm) and was found to be almost comparable in sensitivity. The measurement results for the long-cooled Ågesta fuel (1200 MWd/t U, 31-year-cooled) are shown in Figure 18 using both camera systems. It is apparent from the prototype camera image that it has higher resolution and lower noise. The count rate was also higher for the prototype camera. Nevertheless, it was still possible to verify this long-cooled fuel using the DCVD.

The DCVD was operated at 15 frames a second and binned 2 x 2 for optimum scanning performance. When an image was saved, the detector was set for the highest resolution (1 x 1 binning) and time exposures from 1 to 8 seconds to obtain good statistics. This was satisfactory for most operations. It is still desirable to have even higher frame rates for fast scanning purposes. Andor Technology has indicated that they are working on a 10 MHz ADC system, which should be available soon. In addition, we expect Andor will develop a

back-thinned, EMCCD, 512 x 512 chip that could have a lumogen coating to provide an ultraviolet light efficiency as high as 35%. This efficiency is 4 times that of the present camera. Larger CCD chips with the same architecture are anticipated.

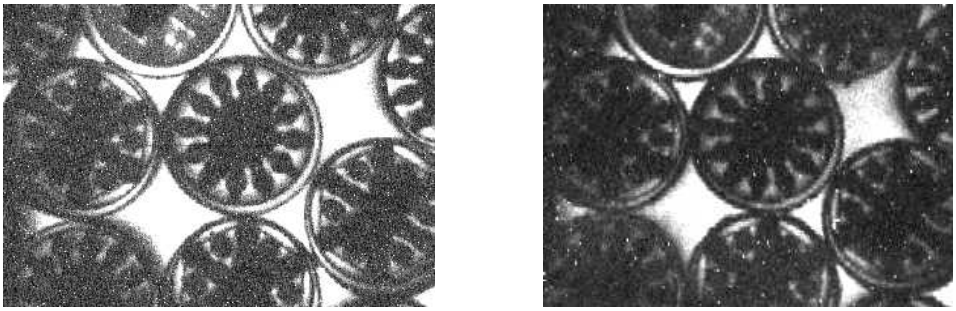

(a) 2 x 2 bin, 5 second exposure (b) 2 x 2 bin, 8 second exposure

*Figure 18: Ågesta fuel assembly*

## 5 CONCLUSION

The new 5 MHz DCVD was successful in measuring the long-cooled Ågesta fuel with a burnup of 1200 MWd/t U and a cooling time of 31 years, which is well below the target of 10 000 MWd/t U and 40 years cooled. Scanning of fuel assemblies was successfully achieved and with the aid of a laser pointer system, random verification was performed in a reasonable time frame.

## 6 ACKNOWLEDGEMENTS

The authors would like to express their gratitude to the Swedish Nuclear Fuel and Waste Management Company (SKB), owners of the Swedish Central Interim Storage for Spent Fuel (CLAB), for making this study possible. We would like to thank the staff members for assistance in planning the tests. The Swedish Support Program and the Canadian Safeguards Support Program funded these tests for the International Atomic Energy Agency.

## 7 REFERENCES

1 J.D. Chen, L. Hildingsson, O. Trepte, E.M. Attas, G.R. Burton and G.J. Young, "Development of a high sensitivity Cerenkov viewing device: Concept SCCD field tests in Sweden"; CSSP Report 88; May 1996.

2 O. Trepte, L. Hildingsson, J.D. Chen, G.R. Burton, G.J. Young and E.M. Attas, "Development of a high sensitivity Cerenkov viewing device: Field test at Ringhals 2 PWR facility, Sweden"; SKI Report 94:45; October 1996.

3 J.D. Chen, E.M. Attas, G.R. Burton, G.J. Young, L. Hildingsson and O. Trepte, "Development of a high sensitivity Cerenkov viewing device: Concept SCCD CVD summary report"; CSSP Report 91; October 1996.

4 J.D. Chen, A.F. Gerwing, P.D. Lewis, M. Larsson, K. Jansson, B. Lindberg, E. Sundkvist, M. Ohlsson, "Development of a high sensitivity digital Cerenkov viewing device: Prototype digital Cerenkov viewing device field test in Sweden"; CSSP Report 123, SKI Report 01:8; May 2002.